Optimal strictly localized basis sets for noble metal surfaces

Sandra García-Gil,[1] Alberto García,[2] Nicolás Lorente,[1] and Pablo Ordejón[1]
[1]*Centre d'Investigació en Nanociència i Nanotecnologia-CIN2 (CSIC-ICN), Campus UAB, 08193 Bellaterra, Spain*
[2]*Institut de Ciència de Materials de Barcelona, CSIC, Campus UAB, 08193 Bellaterra, Spain*
(Received 24 November 2008; revised manuscript received 19 January 2009; published 26 February 2009)

The properties of the (111) surfaces of Cu, Ag, and Au are evaluated using a first-principles approach with strictly localized basis sets. These surfaces present metallic and extended properties that are *a priori* difficult to describe with a local-basis approach. We explore methodologies to enhance the basis sets of the surface atoms in order to accurately describe surface properties such as surface energies, surface states, and work functions. In this way, the advantages of local-basis computations (namely, efficiency, optimum size scaling, and a natural description of bonding in real space) can be retained, while keeping the accuracy in the description of the properties of the surface at a very good level.

DOI: 10.1103/PhysRevB.79.075441 PACS number(s): 73.20.At, 71.15.Ap

I. INTRODUCTION

The surfaces of noble metals have been widely studied as prototypical metallic surfaces. In recent years the number of works that focus on these surfaces has increased greatly due to the ability to manipulate and characterize the surfaces and adsorbed species provided by the scanning probe microscopies, and most notably the scanning tunneling microscope (STM). Noble metal surfaces are ideal for techniques like STM due to their metallic character and reduced chemical reactivity. Also, the existence of surface states in some of these surfaces, such as the (111), which are decoupled from the bulk states and form a quasi-two-dimensional nearly free electron gas, provides a wide variety of effects. For instance, these states can interact with point defects and step edges on the surface, producing standing-wave patterns that can be directly measured with STM.[1,2] These standing waves can also be confined within quantum corrals[3–5] and quantum drums.[6]

The interaction of adsorbates with these surfaces is also a topic of great current interest. One limiting case is the adsorption of individual atoms. For magnetic species, the interplay between the localized magnetic moment of the adsorbate and the delocalized conduction electrons, both at the bulk and surface bands, leads to exciting effects such as Kondo resonances at low temperatures. The observation of these resonances by means of the STM is a very active area,[7–11] with cross-links with the previously mentioned works on surface standing waves, such as the formation of "quantum mirages" in quantum corrals with a magnetic impurity inside.[5,12] The opposite limit is the adsorption of large organic molecules.[13–17] In this case, the interest in using noble metal surfaces is that, due to the filled *d* shell, the density of states at the Fermi level is reduced, compared to the surfaces of transition metals. This makes the noble metal surfaces less reactive toward organic molecules, which generally leads to nondissociative adsorption, often in the physisorption regime. The metallic character of the surface allows the use of STM and related techniques such as scanning tunneling spectroscopy (STS) to study the electronic properties of single molecules weakly coupled with the surface, due to the relatively weak surface-adsorbate interaction. Interestingly, the adsorption on these surfaces of organic molecules containing magnetic atoms also leads to Kondo phenomena.[18,19] Also, the manipulation of single molecules, the excitation of vibrational modes, and the induction of chemical reactions by means of the STM current are active topics of research,[20,21] in which noble metal surfaces are most commonly used as substrates.

Many of these experiments can benefit greatly from the basic understanding provided by first-principles calculations. One clear example is the interpretation of STM images and STS spectra, which is often very difficult without the reference provided by simulated images from electronic structure calculations. Density-functional theory (DFT) (Ref. 22) provides a practical way to compute ground-state properties of systems with significant complexity and number of atoms, as those described here. However, the computational cost of DFT methods is still quite significant and can become prohibitive for systems with a few hundreds of atoms, especially for structural optimizations or molecular dynamics runs for long simulation times. In this context, methods based on strictly localized atomic orbitals have been proposed as an optimal choice for speeding up and reducing the computational cost of DFT calculations.[23–27] These basis functions have the form of atomic orbitals, but are forced to be zero beyond a given confinement radius. The computational savings, compared to standard plane-wave (PW) calculations or other localized bases such as Gaussians, come from several facts. Compared to PWs, the main advantages of strictly localized orbitals are as follows: (i) the number of basis functions is drastically reduced (although the computational effort per basis function to compute the Hamiltonian is lower in PW calculations); (ii) the calculation of the Hamiltonian can easily be made to scale linearly with the number of electrons in the system,[24,28,29] compared to the superlinear scaling in PW calculations,[30] and (iii) the vacuum is described essentially cost-free with strictly localized orbitals, while it is as costly as the space occupied by the atoms in PW calculations (a clear disadvantage for calculations involving surfaces). Compared to other types of localized atomiclike orbitals (such as Gaussians), strictly localized atomic orbitals have the advantage of the straightforward sparsity of the Hamiltonian matrix, without having to impose tolerance cut-

offs, which in solids easily leads to ill-conditioning and numerical instabilities.

When using strictly localized atomic orbitals for the description of solid surfaces, an important issue is whether the basis set is good enough to describe the surface region, and in particular, the decay of the wave functions into the vacuum. This is very important in describing correctly physical properties such as the work function, the energies of surface states, and the interaction of the surface with adsorbed species (especially if weak interactions are involved).[31,32] In the simulation of STM images, it is essential to have a correct description of the decay of the wave functions at points relatively far from the surface and of its dependence with the energy of the state.

In this paper we analyze the accuracy of strictly localized atomic orbital bases to describe the physical properties of the (111) surface of the noble metals Cu, Ag, and Au. We will show that the standard bases commonly used for bulk systems are not sufficiently complete to describe accurately the surface energy, work function, energies of surface states, and the decay of the wave functions into the vacuum. This is partly due to their relatively short localization radii, which are optimal for the description of the bulk system. Increasing the orbital cutoffs at the surface greatly improves the description of the surface properties. However, we will show that better results can be obtained improving the flexibility and range of the orbitals by augmenting the standard bases with either diffuse orbitals centered on the surface atoms or with floating orbitals centered above the surface atomic layer. The paper is organized as follows. In Sec. II we give a description of the calculation method and the structural models used in our studies. Section III describes the form of the strictly localized basis sets used, their optimization and augmentation to describe surface properties. In Sec. IV we present and discuss the results obtained for several physical properties such as surface energies, work functions, position of the surface states and wave function decay into the vacuum, as a function of the basis set used. Finally, in Sec. V we summarize the results of our study and give our concluding remarks.

II. METHODOLOGY

The purpose of this study is to assess the suitability of strictly localized atomic orbital bases to study the surface properties of noble metals. Our strategy is to compare the results obtained with these bases with reference calculations in which all the underlying approximations are the same, but which use essentially converged basis sets. Since we will use pseudopotentials to remove the core electrons, we choose our reference to be the results of well converged PW calculations, which can be made as accurate as needed by just increasing the energy cutoff of the PW expansion of the wave functions.

Our local orbital calculations are done using the SIESTA code,[28,29] whereas the PW results are obtained with the ABINIT code.[33] In both cases, we use the same exchange-correlation functional: the PBE (Ref. 34) form of the generalized gradient approximation (GGA). We also use the same pseudopotentials for both calculations. These are nonlocal norm conserving scalar relativistic pseudopotentials of the Troullier-Martins form.[35] For the three noble metals (Cu, Ag, and Au), the pseudopotentials were generated using the s^1d^{10} electronic configuration of the atom. The radii (in bohr) for the s, p, d, and f components of the pseudopotential were 2.05, 2.30, 1.75 and 2.05 for Cu, 2.30, 2.30, 1.80 and 2.30 for Ag, and 2.35, 2.35, 2.35 and 2.35 for Au. The pseudopotentials were expressed in the full nonlocal Kleinman-Bylander form,[36] and the same local and nonlocal components were used in the SIESTA and ABINIT calculations.[37] Therefore, the two calculations only differ in the type of basis set used.[38]

III. STRICTLY LOCALIZED BASIS SETS

In this section we describe the strictly localized basis sets. We will first describe the standard basis sets that are commonly used, how they are obtained and optimized. Then, we will propose schemes to augment them to describe accurately the surface properties.

We use basis sets made of strictly localized numerical atomic orbitals. This implies orbitals that are a product of a numerical radial function with a finite confinement radius[23] and a spherical harmonic. The standard machinery of quantum chemistry[39] (multiple-ζ, polarization, floating, contracted and diffuse orbitals) can be used to define the number of radial functions for each angular momentum component (and their shape) and the maximum angular momentum of the basis.[40] The main difference between the orbitals used here and the standard bases in quantum chemistry (such as Gaussians or Slater orbitals) is that our radial functions are numerical orbitals (and therefore have no predefined functional shape), and are strictly zero beyond a given radius (see Fig. 1 and text below).

A. Basis sets optimized for the bulk

For bulk calculations, basis sets obtained using the multiple-ζ plus polarization scheme[39] usually provide excellent performance. Typically, a double-ζ basis with a single polarization shell (denoted as DZP basis) is sufficient to produce results very close to convergence.[26] "Double-ζ" stands for the use of two radial functions (with different radial shape) for each angular momentum component corresponding to the occupied shells of the free atom. In the case of the noble metals, this amounts to using two radial functions for the valence s shell and two radial functions for the valence d shell. The polarization orbitals serve to describe the distortion of the valence orbitals due to bond formation, and using a single radial function is usually enough. In the case of the noble metals, the polarization orbitals would consist in a single shell of p orbitals (which serves to polarize the s shell), and eventually a shell of f orbitals (to polarize the d shell). However, the effect of the f polarization orbitals is very small, so they are usually not included in the basis. Therefore, for the noble metals, the DZP basis consists of 15 orbitals: two shells of s functions (two orbitals), two shells of d functions (ten orbitals), and one shell of polarization p functions (three orbitals).

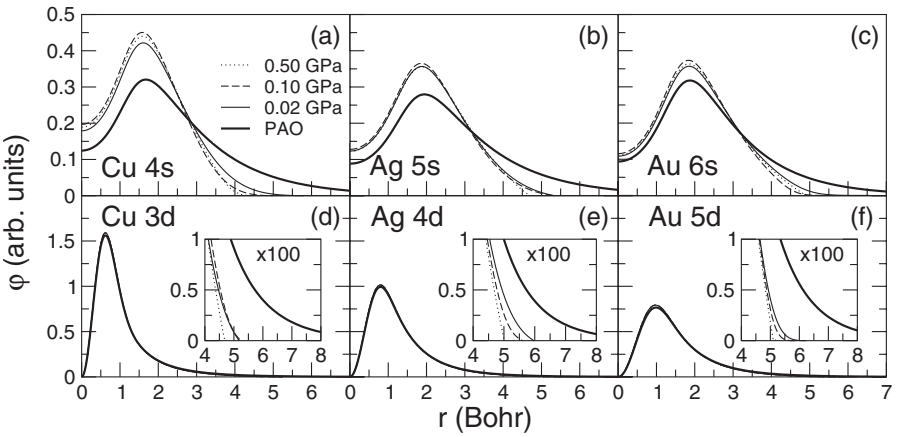

FIG. 1. Radial function for the first-ζ orbitals of the s (top) and d (bottom) shells of Cu, Ag, and Au. We show the orbitals optimized in the bulk for three different values of the fictitious pressure (0.5, 0.1, and 0.02 GPa), as well as the pseudoatomic orbital (PAO), which is the solution of the free atom with open boundary conditions.

Choosing the shape of the numerical radial functions for each orbital can be done in several ways. Here, the first-ζ orbital for each angular momentum shell is obtained from the solution of the free atom (with the same pseudopotential), while the second ζ is obtained from the first one using the "split valence" scheme proposed by Artacho *et al.*[40] for numerical atomic orbitals.[41] The strict localization of the orbitals is achieved by adding a smooth confining potential that diverges at r_c (the chosen cutoff radius of the orbital) when we solve the free atom.[26]

In general, choosing the localization radii r_c for each of the orbitals in the basis set is a delicate issue. Larger radii usually provide better quality bases (i.e., lower energies), but at the cost of increasing the computational effort. Different orbitals and chemical species have different decay properties, and therefore different confinement radii should be used. Besides, the optimal shape (and therefore the confinement radius) of a given orbital may change depending on the chemical environment. Anglada *et al.*[42] developed a method to obtain optimal values of r_c for all the orbitals in a given reference system, in such a way that the choice of confinement versus basis quality can be tailored at will for that specific reference system. In particular, the confinement radii (as well as other possible parameters which define the basis sets, such as the smoothness of the confining potential, the matching radii of the second-ζ orbitals, net atomic charges, etc.) are chosen to minimize a fictitious enthalpy, defined as $H=E+PV$, where E is the total energy of the reference system, $V=(4\pi/3)\Sigma_\mu r_{c\mu}^3$ is the sum of volumes of the basis orbitals ϕ_μ, and P is a fictitious pressure parameter. By varying P, we can tailor the quality/confinement of the basis: by choosing a small pressure, the main contribution to the enthalpy is the energy, and therefore the radii tend to become larger to produce lower energies; for large values of the pressure, the volume of the orbitals has a high weight in the enthalpy, and minimization of the latter leads to orbitals with smaller radii, at the expense of increasing the energy of the system.

In this work, we have optimized the basis sets for the bulk using the method sketched above. We have used three different pressure values (0.5, 0.1, and 0.02 GPa) to obtain bases with different confinement radii. The parameters obtained for each pressure for Cu, Ag, and Au are shown in Table I. We see that the expected trends (larger radii for smaller optimization pressure) are obtained. In Table II we present the bulk properties obtained with these bases for the three noble met-

TABLE I. Parameters defining the basis sets for Cu, Ag, and Au optimized in the bulk, for three different values of the fictitious pressure (0.5, 0.1, and 0.02 GPa). r_c is the cutoff radius of each of the orbitals. V_0 and r_i are parameters which determine the confining potential for each shell (see Ref. 26). Q is a net charge assigned to the atom in the computation of the first-ζ orbital by solving the free atom problem (see Ref. 26).

		r_c (bohr)					V_0 (Ry)			r_i (bohr)			
	Basis	$s_{1\zeta}$	$s_{2\zeta}$	p	$d_{1\zeta}$	$d_{2\zeta}$	s	p	d	s	p	d	$Q(e)$
Cu	0.5 GPa	4.38	1.55	4.86	4.75	2.62	49.9	4.0	78.9	3.32	2.13	4.53	0.074
	0.1 GPa	4.95	1.71	5.38	5.22	3.17	23.6	6.6	14.9	2.26	1.63	3.96	0.074
	0.02 GPa	5.77	2.19	5.49	5.21	2.92	19.0	5.1	5.2	1.94	0.26	2.80	0.074
Ag	0.5 GPa	4.71	1.40	5.29	5.06	2.76	13.4	4.3	74.6	3.55	3.55	4.92	0.080
	0.1 GPa	5.33	2.67	5.52	5.62	3.21	6.7	3.4	19.4	2.11	1.98	4.09	0.080
	0.02 GPa	5.37	3.33	5.98	5.97	4.01	4.4	5.3	6.4	2.09	1.86	3.36	0.079
Au	0.5 GPa	4.99	1.32	5.00	5.15	1.93	160.4	108.1	236.8	4.76	4.84	5.02	0.025
	0.1 GPa	5.53	3.69	6.09	5.87	2.30	104.8	66.7	125.3	3.84	4.72	4.47	0.025
	0.02 GPa	6.52	4.18	6.90	6.18	2.35	99.0	54.3	54.3	3.76	3.96	4.11	0.025

TABLE II. Bulk properties of Cu, Ag, and Au for the basis sets optimized in the bulk with three different values of the fictitious pressure (0.5, 0.1 and 0.02 GPa). The results from PW calculations and from experiments (taken from Ref. 45) are also shown. a_0: equilibrium lattice constant. B: bulk modulus. ΔE: total energy per atom, relative to the PW result.

		Basis				
		0.5 GPa	0.1 GPa	0.02 GPa	PW	Exp
Cu	a_0(Å)	3.63	3.65	3.67	3.67	3.61
	B(GPa)	178	164	128	134	137
	ΔE(eV)	0.19	0.06	0.04	0.0	
Ag	a_0(Å)	4.12	4.16	4.17	4.17	4.09
	B(GPa)	112	101	97	86	101
	ΔE(eV)	0.21	0.05	0.03	0.0	
Au	a_0(Å)	4.14	4.17	4.18	4.16	4.08
	B(GPa)	199	161	158	140	173
	ΔE(eV)	0.39	0.20	0.16	0.0	

als and compare them with the results from PW calculations. In all cases, the lattice constant is very well described, with differences between the local orbitals and the PW results which are much smaller than the difference with the experimental values. The total energies per atom obtained with the localized orbitals are very close to those of PWs, but slightly higher, since the calculations are variational and the PW results shown are essentially converged. The quality of the local orbital bases improves with increasing their cutoff radii (i.e., decreasing the fictitious pressure). For the smallest optimization pressure (0.02 GPa), corresponding to the longest radii considered here, the total energies are nearly equal to the PW results,[38] reflecting the fact that DZP bases are excellent to describe bulk structures.[26] Further reducing the fictitious pressure below 0.02 GPa does not modify the results significantly (e.g., changes in the energy are less than 0.01 eV).

It is interesting to analyze the shape and confinement radii obtained for the basis sets optimized in the bulk. In Fig. 1 we show the first-ζ orbitals of the s and d shells of the three elements as an illustration. The shapes of the orbitals optimized with different pressures are very similar (especially for the d shell), although the tails are longer for smaller optimization pressures, as expected. However, basis sets obtained by optimization in the bulk using even lower values of the fictitious pressure do not have significantly bigger orbitals than those obtained for 0.02 GPa. The reason is that the total energy of the bulk system is not significantly reduced by further increasing the radii of the orbitals, because the presence of the basis of neighboring atoms makes the long tails in the atomic orbitals unnecessary. This is in contrast to the situation for the free atom, where an optimization of the basis with decreasing values of the pressure produces orbitals with increasing radii, until the true exponentially decaying (Slater-type) pseudoatomic orbitals (PAO's) are obtained. These PAO's are also shown in Fig. 1, where it is clear that the orbitals optimized in the bulk adapt to the environment by modifying their shape and range and, in general, becoming more localized than in the free atom. This is especially pronounced for the s shell, for which the compression and suppression of the long atomic tail is very strong. For the d shell, the overall shape of the bulk orbitals is essentially the same as that of the PAO, although the tail is also suppressed. Despite the more compact nature of the d orbitals compared to the s states, the optimum radii for both shells are quite similar for the three elements, for all the pressures considered. This has been already observed in bulk transition metals like Fe.[43] Also, the optimal radius for the d shell is, in general, less dependent on the fictitious pressure than that for the s shell. Both observations are related to the known fact that outer shells of atoms are more compressible than inner shells.[44]

In summary, basis orbitals optimized in the bulk, even with very small fictitious pressures, do not have the long tails that will be needed to describe surface properties, as we will see below. Besides, the use of the orbitals optimized in the free atom to describe the surface properties is not an optimal solution either, since the decay rate of the wave functions in the atom and in the surface will be different. Therefore, schemes to improve the basis at the surface will be necessary. In the following we explore some possible schemes to achieve this.

B. Basis sets for surfaces

To describe accurately the properties of the surfaces, we need to include orbitals with weight in the vacuum region, which can describe the long decay of the wave functions. This can be done in several ways. Here we explore a number of possibilities, which are schematically shown in Fig. 2.

The first scheme we have explored is simply to increase the radius of the orbitals of the atoms at the surface layer, which allows the wave functions to spread further into the vacuum [see Fig. 2(a)]. For simplicity, we only show here the results of enlarging the radius of the first-ζ orbital of the s shell, since we have observed that increasing the radii of the rest of the orbitals only has a minor effect on the surface properties. The confinement radii were taken as a variational parameter to optimize the quality of the basis and are chosen to minimize the surface energy of the (111) surface. We will

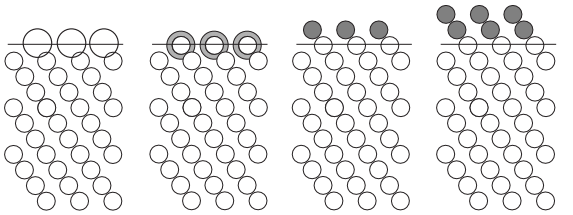

FIG. 2. Schematic view of different schemes for basis sets for the surface. The atomic positions follow the fcc stacking sequence. The lines indicate the position of the surface layer. In all panels, small open circles represent the basis optimized in the bulk. In (a) the atoms at the surface layer have a DZP basis, but the cutoff radii are enlarged compared to the bulk (shown as large open circles). In (b) the surface atoms are described by a bulk DZP basis, plus an augmentation *s* orbital centered at the surface atoms, indicated by large gray circles. In (c) and (d) one and two layers of floating orbitals (shown by the small gray circles) are located above the surface, respectively.

refer to these DZP bases with expanded *s* orbitals as "Opt. DZP" bases. For Cu, Ag, and Au we obtain values for the *s* orbital cutoff of 12, 10, and 16 bohr, respectively. These are significantly larger than the values obtained for the bulk, which clearly shows the need to expand the basis to describe properly the vacuum region. It should be noted, however, that increasing the orbital localization cutoff of the DZP basis leads to basis functions with the natural decay of the atomic orbitals in the free atom. On the other hand, in a crystal surface each wave function will fall into the vacuum with a different decay rate, which depends on the energy of the state. Therefore, we should expect that these Opt. DZP bases, while performing better than the bulk DZP basis to describe surface properties, will not be flexible enough, and that including more orbitals with different decay rates or with weight on more distant regions from the surface will be necessary. We next explore some possible schemes to achieve this.

The second scheme is to include in the basis set centered on the atoms a shell of diffuse functions, with longer cutoff and slower decay than the bulk DZP orbitals [see Fig. 2(b)]. We only include a set of atom-centered orbitals with *s* symmetry, and only for the atoms at the surface. For the radial shape, we used the first excited state of *s* symmetry for the free atom, confined within a given cutoff radius. These orbitals have one node, in order to be orthogonal to the valence *s* orbital. In Fig. 3 we show the example of the diffuse orbital for Ag, which has a large weight at large distances, where the valence 5*s* orbital is null. Again, we choose the confinement radii that minimize the surface energy of the (111) surface, and find that the optimal radius for the diffuse orbitals is around 7 bohr for Cu and 9 bohr for Ag and Au. Reducing the radii from these optimal values rapidly increases the surface energy, since the wave functions are again too much confined. Using longer radii increases the energy slightly, by up to 30–40 meV above the value for the optimal radius, and brings a considerable increase in the computational effort. The results reported in the next section are obtained using the optimized values for the cutoff radii of the diffuse orbitals.

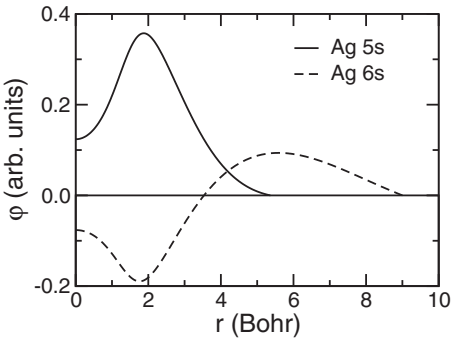

FIG. 3. Radial part of the first-ζ orbital of the 5*s* shell (full line) and the diffuse 6*s* orbital of the surface atoms (dashed line) for silver.

The last scheme we consider is to add a set of floating orbitals located above the surface.[46,47] These are off-site orbitals centered at points where there are no atoms. We only include floating orbitals of *s* symmetry, with the same radial shape and cutoff radius as the valence *s* orbital of the basis set of the atoms at the surface. We have considered two options for the location of the floating orbitals: (i) using one layer of orbitals, centered at the positions which the next layer of atoms would have above the surface in the crystal [see Fig. 2(c)], and (ii) using two layers of orbitals, centered at the next two atomic layers above the surface [see Fig. 2(d)]. Obviously, the second option produces a richer, more flexible basis set.

IV. RESULTS AND DISCUSSION

In this section we present the results obtained for the properties of the (111) surface of the three noble metals, for the different basis sets described in the previous section. All the surface calculations are done using a slab geometry with 18 atomic layers and a vacuum of 14 Å thickness. We found that these slabs are thick enough so that the splitting of the surface state (due to the interaction between the states at both surfaces of the slab) is of the order of a few tens of meV. We will compare the electronic properties obtained with different basis sets for the same geometries. Since the surface relaxations are very small in these systems, we have used the geometry of the unrelaxed surfaces (i.e., with the atoms at the bulk positions). We have done this for two different values of the lattice constant: the experimental and the one that minimizes the bulk energy in the DFT calculation. Since the conclusions obtained are the same, here we will only present the results obtained at the experimental lattice constant.

A. Energies

Figure 4 shows the values for the surface energies (in eV per surface atom) for each of the basis sets considered, calculated by subtracting bulk and slab total energies: $E = 1/2(E_{\mathrm{slab}} - NE_{\mathrm{bulk}})$, where N is the number of atoms in the slab, and E_{bulk} is the bulk energy per atom. The factor of 2 accounts for the two surfaces in the slab. We see that the DZP basis set optimized for the bulk produces values which

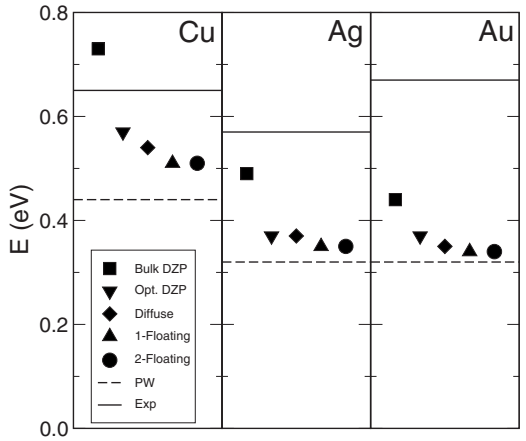

FIG. 4. Surface energies (eV per surface atom) obtained with different basis sets. Experimental values taken from Ref. 48.

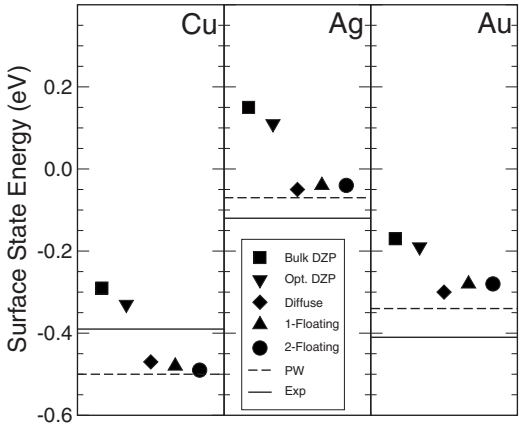

FIG. 6. Energy of the surface state at the Γ point, with respect to the Fermi energy, obtained with different basis sets. Experimental values taken from Ref. 50.

are far too high compared to PW results. Increasing the radii of the *s* orbitals of the surface atoms (Opt. DZP basis) already reduces the differences by a factor of 2 or more. Inclusion of a shell of diffuse orbitals in the surface atoms produces slightly better energies, while including floating orbitals gives results very close to those of PW calculations. Including one or two layers of floating orbitals produces nearly identical results. For Ag and Au, the floating orbitals bases give results within 0.03 eV of the PW ones. For Cu, the differences are larger (about 0.07 eV) and we have found that further reducing this difference requires an increase in the radius of the polarization *p* orbitals of the surface atoms.

We compute the work function by plotting the electrostatic potential profile along the direction perpendicular to the surface and taking its value in the vacuum region with respect to the Fermi level. The results are shown in Fig. 5. Again, the DZP basis optimized in the bulk produces large deviations with respect to the PW results: the values are significantly smaller, up to a factor of 2 for Cu. For the improved bases we find the same trends as for the surface energy: (i) increasing of the radius of the *s* orbitals reduces the errors to about a half, (ii) the results improve for the diffuse orbitals, and (iii) floating orbitals produce the best results, in

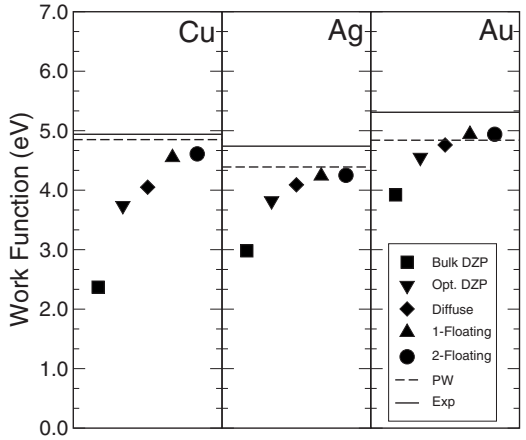

FIG. 5. Work function obtained with different basis sets. Experimental values taken from Ref. 49.

agreement with the PW values within 0.1 eV. We should note that the calculation of the work function is a very delicate task, especially in the case of PWs, since small deviations from self-consistency and small errors in the charge density at the vacuum region easily lead to deviations of several tenths of an electron volt in the computed values. As for the case of the surface energies, we see that addition of more than one layer of floating orbitals does not produce significant changes in the values of the work function.

The unreconstructed (111) surfaces of noble metals exhibit the presence of Shockley surface states[50] at the projected bulk *sp*-band gap at the center of the surface Brillouin zone (SBZ). These states have a parabolic dispersion with the minimum at the Γ point of the SBZ. Figure 6 shows the position of the minimum of the surface band for each basis set. Once again, the bulk-optimized DZP bases are not sufficient to describe properly these states: they yield surface state energies which are significantly higher than those of the PW results. This is due to the fact that the bulk basis sets decay too fast to describe properly the surface state decay, which extends into the vacuum considerably. Therefore, the surface state wave functions are too confined, which is reflected in an increased energy. However, in contrast with the calculation of the surface energy and the work function, increasing the radius of the *s* orbitals of the surface atoms does not produce a significant improvement on the computed surface states energies. As we discussed in Sec. III B, the orbitals computed in the atom have the natural decay of the atomic wave function, which is different from that of the bulk and surface wave functions (see below), and this has a clear impact on the computed surface energies. Including orbitals with higher weight in the vacuum region improves the situation dramatically. Both the diffuse and floating bases produce surface state energies within 50 meV of the PW results. Once again, including more than one layer of floating orbitals does not provide an appreciable improvement.

B. Wave functions

We now turn to the study of the decay of the wave functions into the vacuum. This is obviously a very important

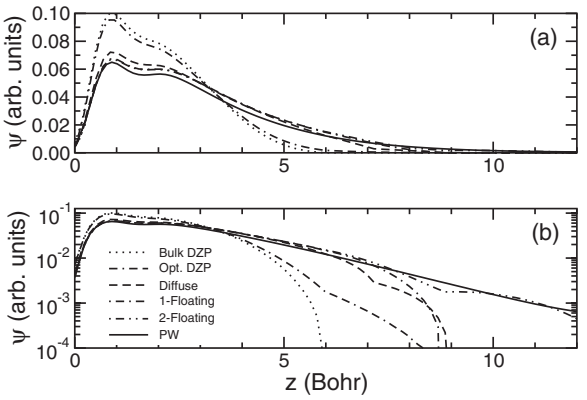

FIG. 7. Decay into the vacuum of the wave function of the surface state at the Γ point for Ag, plotted along a line in the z direction (perpendicular to the surface) which passes through a surface atom. The last atomic layer is located at $z=0$. (a) and (b) show the wave function in linear and logarithmic scale, respectively.

issue in the quantitative description of STM images. The exponential decay into the vacuum can be well described when PWs are used as basis sets, but it is questionable whether finite range atomic orbitals can also describe it properly, at least in a qualitative manner. It should be noted, however, that even PW techniques find difficulties in describing accurately the wave functions at relatively long distances from the surfaces, since they contribute negligibly to the total energy, which is the variational target of the wave function optimization. Here, we explore the quality of our finite-range atomic orbitals to describe the decay of the wave functions at distances from the surface halfway the typical STM tip-sample distances of 5–10 Å. We will focus on wave functions which are located near the Fermi level (which are the ones relevant for the STM process), and in particular on those corresponding to the surface state at the Γ point. We will only describe the results for silver, since those for copper and gold are very similar.

The decay into the vacuum for the wave function of the surface state of silver, along a line perpendicular to the surface passing through a surface atom and through a hollow site, is shown in Figs. 7 and 8, respectively. The abscissa indicates the depth into the vacuum, with the origin located

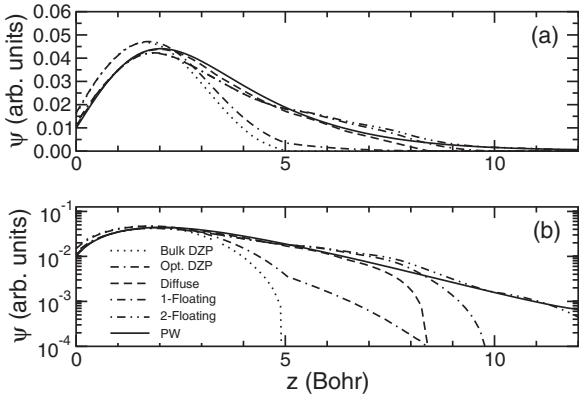

FIG. 8. Same as in Fig. 7, plotted along a line passing through a surface hollow site.

at the position of the last atomic layer of the slab. The basis sets optimized for the bulk are certainly not sufficiently extended to reproduce the decay of wave functions at energies near the Fermi level. This is shown here for the surface state, but it is also true for the other bulk states at similar energies. Increasing the radius of the s orbitals of the surface atoms produces some improvement, mainly extending the wave function further into the vacuum, but the obtained decay rate at long distances from the surface is quite different from that obtained with plane waves. This is again due to the different natural decay of the atomic wave functions compared with those of the surface. However, the augmented bases are able to reproduce quite closely the results from PWs, up to distances close to 9 bohr. Both diffuse orbitals and a single shell of floating orbitals produce comparable results, with wave functions which reproduce quite well the PW results, but decay abruptly to zero at around 9 bohr from the surface. Including a double shell of floating orbitals improves dramatically the description above 10 bohr. Clearly, an accurate calculation of the wave function at even larger distances could be done by further increasing the number of shells of floating orbitals above the surface.

With any of the localized orbital bases, the discreteness of the basis set is apparent in the wave function plots: while the PWs are able to follow very well the expected exponential behavior (linear shape in logarithmic scale), the wave functions expanded in local orbitals show bumps which depart from the exponential decay, and which are due to the expansion in a finite (and small) number of orbitals with fixed, nonexponential shape. However, the overall form of the wave functions follows quite remarkably the expected decay. Except at the distance where the localized orbitals drop to zero (because of their confinement), the wave functions follow a nearly exponential behavior, with a slope in close agreement with that of the PW results for all the augmented bases considered here.

V. SUMMARY AND CONCLUSIONS

In summary, we have analyzed the quality of strictly localized atomic orbital basis sets to describe the properties of the (111) surface of noble metals. We found that basis sets optimized for the bulk are not able to provide sufficient accuracy for many purposes. In particular, these bases produce surface energies that are too high, as it is also the case with the energies of the surface state, while the work functions are underestimated. The decay of the wave functions close to the Fermi level is too fast, not being able to reproduce the exponential decay at distances longer than 2–3 bohr.

Increasing the range of the s orbitals of the surface atoms yields important improvements in the computed surface energies and work functions. However, these enlarged bases are still not sufficiently accurate to describe the energy of the surface states and the form of their decay into the vacuum due to their intrinsic decay rate following the shape of the orbitals in the free atom.

Augmentation of the local orbitals basis sets with either a shell of diffuse orbitals in the surface atomic layer, or with one or two shells of floating orbitals in the vacuum region, is

shown to produce a dramatic improvement both in the energies and in the wave function decay shape. The best results are obtained with a double shell of floating orbitals, for which the wave functions follow closely the PWs results up to distances larger than 10 bohr from the surface. For the energetics, floating orbitals provide slightly better results than diffuse orbitals, although the differences are small. In any case, the errors in energies (surface energy, work function, and surface state energy) for any of the augmented bases tested here are always below 0.1 eV (and often much smaller).

Let us now comment on the computational cost of the different bases presented here. The main part of the CPU time is split between the calculation of the Hamiltonian matrix (mostly in the real-space numerical integrals)[29] and the solution of the eigenvalue problem. In our slab calculations with 18 atomic layers, the latter is nearly equally costly for all the schemes presented here, since the total number of orbitals is almost the same: for each surface, there is only one extra function in the case of diffuse orbitals and one shell of floating orbitals, and two extra functions for the case of two shells of floating orbitals. These are negligible numbers, compared with the total number of orbitals in an 18-layer slab (270 for the DZP basis). However, the calculation of the Hamiltonian matrix is significantly more expensive for orbitals with large confinement radii, because both the number of integrals to be computed and the number of points in real space needed to compute them increase dramatically with the orbital radii. As a consequence, the Opt. DZP basis has the largest computational cost of all those considered here, since it contains very long orbitals, with an overhead of the order of 100% compared to the bulk optimized basis. The diffuse orbitals basis has a smaller overhead, of roughly 20% over the bulk optimized basis. Finally, the bases with floating orbitals have a negligible overhead of a few percent over the bulk optimized bases, since they have orbitals with small confinement radius.

The favorable cost and the accuracy provided by the floating orbitals basis make them the preferred choice for calculations of the properties of free surfaces. On the other hand, in the study of molecules adsorbed on surfaces, and especially for weakly interacting species, the use of floating orbitals can be problematic, since they could overlap with the molecular basis. Also, in simulations involving dynamics and relaxations, moving the centers of the floating orbitals can lead to instabilities. In these cases, the preferred basis would be the one including diffuse functions, since it provides very good accuracy and only a minor overhead in computational effort. The DZP bases optimized in the surface are not found to be optimal neither for accuracy nor for computational efficiency.

In conclusion, we have shown that augmentation of the standard strictly localized orbital basis sets leads to a very good description of the properties of the surfaces of noble metals. This work provides a practical way[51] to study problems involving these surfaces at a significantly reduced cost compared to PW calculations, while retaining a very acceptable level of accuracy. Work is underway in using these bases to study several problems regarding adsorption of large organic molecules and the simulation of STM images on these surfaces.

ACKNOWLEDGMENTS

This work was supported by Spanish MEC (Grants No. FIS2006-12117-C04-01 and No. CSD2007-00050) and Generalitat de Catalunya (Grant No. SGR-2005 683). We thank J. Junquera for useful discussions and for making the pseudopotential translation code available. This work was done using the computing facilities of CESCA and CESGA.

[1] M. F. Crommie, C. P. Lutz, and D. M. Eigler, Nature (London) **363**, 524 (1993).
[2] Y. Hasegawa and Ph. Avouris, Phys. Rev. Lett. **71**, 1071 (1993).
[3] M. F. Crommie, C. P. Lutz, and D. M. Eigler, Science **262**, 218 (1993).
[4] K.-F. Braun and K.-H. Rieder, Phys. Rev. Lett. **88**, 096801 (2002).
[5] G. A. Fiete and E. J. Heller, Rev. Mod. Phys. **75**, 933 (2003) and references therein.
[6] C. R. Moon, L. S. Mattos, B. K. Foster, G. Zeltzer, W. Ko, and H. C. Manoharan, Science **319**, 782 (2008).
[7] V. Madhavan, W. Chen, T. Jamneala, M. F. Crommie, and N. S. Wingreen, Science **280**, 567 (1998).
[8] J. Li, W.-D. Schneider, R. Berndt, and B. Delley, Phys. Rev. Lett. **80**, 2893 (1998).
[9] N. Knorr, M. A. Schneider, L. Diekhoner, P. Wahl, and K. Kern, Phys. Rev. Lett. **88**, 096804 (2002).
[10] N. Néel, J. Kröger, L. Limot, K. Palotas, W. A. Hofer, and R. Berndt, Phys. Rev. Lett. **98**, 016801 (2007).
[11] L. Vitali, R. Ohmann, S. Stepanow, P. Gambardella, K. Tao, R. Huang, V. S. Stepanyuk, P. Bruno, and K. Kern, Phys. Rev. Lett. **101**, 216802 (2008).
[12] H. C. Manoharan, C. P. Lutz, and D. M. Eigler, Nature (London) **403**, 512 (2000).
[13] J. V. Barth, G. Costantini, and K. Kern, Nature (London) **437**, 671 (2005).
[14] A. Hauschild, K. Karki, B. C. C. Cowie, M. Rohlfing, F. S. Tautz, and M. Sokolowski, Phys. Rev. Lett. **94**, 036106 (2005).
[15] R. Otero, M. Lukas, R. E. A. Kelly, W. Xu, E. Laegsgaard, I. Stensgaard, L. N. Kantorovich, and F. Besenbarcher, Science **319**, 312 (2008).
[16] K. J. Franke, G. Schulze, N. Henningsen, I. Fernandez-Torrente, J. I. Pascual, S. Zarwell, K. Ruck-Braun, M. Cobian, and N. Lorente, Phys. Rev. Lett. **100**, 036807 (2008).
[17] N. Gonzalez-Lakunza, I. Fernandez-Torrente, K. J. Franke, N. Lorente, A. Arnau, and J. I. Pascual, Phys. Rev. Lett. **100**, 156805 (2008).
[18] A. Zhao, Q. Li, L. Chen, H. Xiang, W. Wang, S. Pan, B. Wang, X. Xiao, J. Yang, J. G. Hou, and Q. Zhu, Science **309**, 1542 (2005).
[19] V. Iancu, A. Deshpande, and S. W. Hla, Nano Lett. **6**, 820 (2006).

[20] N. Lorente, R. Rurali, and H. Tang, J. Phys.: Condens. Matter **17**, S1049 (2005) and references therein.
[21] M. Galperin, M. A. Ratner, and A. Nitzan, J. Phys. Condens. Matter **19**, 103201 (2007) and references therein.
[22] P. Hohenberg and W. Kohn, Phys. Rev. **136**, B864 (1964); W. Kohn and L. J. Sham, *ibid.* **140**, A1133 (1965).
[23] O. F. Sankey and D. J. Niklewski, Phys. Rev. B **40**, 3979 (1989).
[24] P. Ordejón, E. Artacho, and J. M. Soler, Phys. Rev. B **53**, R10441 (1996).
[25] S. D. Kenny, A. P. Horsfield, and H. Fujitani, Phys. Rev. B **62**, 4899 (2000).
[26] J. Junquera, O. Paz, D. Sánchez-Portal, and E. Artacho, Phys. Rev. B **64**, 235111 (2001).
[27] T. Ozaki, Phys. Rev. B **67**, 155108 (2003); T. Ozaki and H. Kino, *ibid.* **69**, 195113 (2004).
[28] D. Sánchez-Portal, P. Ordejón, E. Artacho, and J. M. Soler, Int. J. Quantum Chem. **65**, 453 (1997).
[29] J. M. Soler, E. Artacho, J. Gale, A. García, J. Junquera, P. Ordejón, and D. Sánchez-Portal, J. Phys.: Condens. Matter **14**, 2745 (2002).
[30] M. C. Payne, M. P. Teter, T. A. Arias, and J. D. Joannopoulos, Rev. Mod. Phys. **64**, 1045 (1992).
[31] R. Rurali, N. Lorente, and P. Ordejón, Phys. Rev. Lett. **95**, 209601 (2005).
[32] K. Lee, J. Yu, and Y. Morikawa, Phys. Rev. B **75**, 045402 (2007).
[33] X. Gonze, J.-M. Beuken, R. Caracas, F. Detraux, M. Fuchs, G.-M. Rignanese, L. Sindic, M. Verstraete, G. Zerah, F. Jollet, M. Torrent, A. Roy, M. Mikami, Ph. Ghosez, J.-Y. Raty, and D. C. Allan, Comput. Mater. Sci. **25**, 478 (2002).
[34] J. P. Perdew, K. Burke, and M. Ernzerhof, Phys. Rev. Lett. **77**, 3865 (1996).
[35] N. Troullier and J. L. Martins, Phys. Rev. B **43**, 1993 (1991).
[36] L. Kleinman and D. M. Bylander, Phys. Rev. Lett. **48**, 1425 (1982).
[37] ABINIT pseudopotentials are translated to SIESTA format by means of a utility developed by J. Junquera, M. Verstraete, X. Gonze, and A. García.
[38] We note that numerical differences between ABINIT and SIESTA (stemming from different numerical algorithms in both codes) reflect in total energies differences of about 0.05 eV/atom, even for converged basis sets (for which the resulting energies should coincide).
[39] S. Huzinaga, J. Andzelm, M. Klobukowski, E. Radzio-Andzelm, Y. Sakai, and H. Tatewaki, *Gaussian Basis Sets for Molecular Calculations* (Elsevier, Amsterdam, 1984); R. Poirier, R. Kari, and R. Csizmadia, *Handbook of Gaussian Basis Sets* (Elsevier, Amsterdam, 1985), and references therein.
[40] E. Artacho, D. Sánchez-Portal, P. Ordejón, A. García, and J. M. Soler, Phys. Status Solidi B **215**, 809 (1999).
[41] The second-ζ functions are defined as the difference between the first-ζ orbital and an orbital constructed to reproduce the tail of the first ζ from a matching radius outward, and to run smoothly inward. Therefore, by construction, the second ζ's have confinement radii equal to the matching radii, and smaller than the ones of the corresponding first ζ's.
[42] E. Anglada, J. M. Soler, J. Junquera, and E. Artacho, Phys. Rev. B **66**, 205101 (2002).
[43] J. Izquierdo, A. Vega, L. C. Balbás, D. Sánchez-Portal, J. Junquera, E. Artacho, J. M. Soler, and P. Ordejón, Phys. Rev. B **61**, 13639 (2000).
[44] J. P. Connerade, P. Kengkan, P. A. Lakshmi, and R. Semaoune, J. Phys. B **33**, L847 (2000).
[45] C. Kittel, *Introduction to Solid State Physics*, 7th ed. (Wiley, New York, 1996) (and references therein).
[46] P. J. Feibelman, Phys. Rev. B **51**, 17867 (1995).
[47] K. Doll, Surf. Sci. **600**, L321 (2006).
[48] F. R. de Boer, R. Boom, W. C. M. Mattens, A. R. Miedma, and A. K. Niessen, *Cohesion in Metals* (North-Holland, Amsterdam, 1988).
[49] H. B. Michaelson, J. Appl. Phys. **48**, 4729 (1977).
[50] S. D. Kevan and R. H. Gaylord, Phys. Rev. B **36**, 5809 (1987).
[51] The basis sets described in this work, for use with the SIESTA code, can be downloaded from http://www.uam.es/siesta